American Mineralogist, Volume 83, pages 390–399, 1998

Georgeericksenite, $Na_6CaMg(IO_3)_6(CrO_4)_2(H_2O)_{12}$, a new mineral from Oficina Chacabuco, Chile: Description and crystal structure

MARK A. COOPER,[1] FRANK C. HAWTHORNE,[1] ANDREW C. ROBERTS,[2] JOEL D. GRICE,[3] JOHN A.R. STIRLING,[2] AND ELIZABETH A. MOFFATT[4]

[1]Department of Geological Sciences, University of Manitoba, Winnipeg, Manitoba R3T 2N2, Canada
[2]Geological Survey of Canada, 601 Booth Street, Ottawa, Ontario, K1A 0E8, Canada
[3]Research Division, Canadian Museum of Nature, P.O. Box 3443, Station D, Ottawa, Ontario K1P 6P4, Canada
[4]Canadian Conservation Institute, 1030 Innes Road, Ottawa, Ontario K1A 0C8, Canada

ABSTRACT

Georgeericksenite, $Na_6CaMg(IO_3)_6[(Cr_{0.84}S_{0.16})O_4]_2(H_2O)_{12}$, space group $C2/c$, a = 23.645(2), b = 10.918(1), c = 15.768(1) Å, β = 114.42(6)°, V = 3707.3(6) Å^3, Z = 4, is a new mineral on a museum specimen labeled as originating from Oficina Chacabuco, Chile. It occurs both as isolated and groupings of 0.2 mm sized bright lemon-yellow micronodules of crystals on a host rock principally composed of halite, nitratine, and niter. Associated minerals include plagioclase, clinopyroxene, and an undefined hydrated Ca-K-Ti-iodate-chromate-chloride. Georgeericksenite crystals average 30 × 5 × 5 μm in size and are prismatic to acicular, elongate along [001] and somewhat flattened on {110}, and they have a length-to-width ratio of 6:1. Forms observed are {100}, {110} major, and {$\bar{2}$33} minor. Crystals are pale yellow, possess a pale-yellow streak, are transparent, brittle, and vitreous, and do not fluoresce under ultraviolet light. The estimated Mohs hardness is between 3 and 4, the calculated density is 3.035 g/cm^3, and the mineral is extremely soluble in cold H_2O. The optical properties of georgeericksenite are biaxial (+) with α = 1.647(2), β = 1.674(2), γ = 1.704(2), 2V_{calc} = +88.4° and the orientation is $Z \approx c$. Pleochroism is slight with X = very pale yellow and Z = distinct yellow-green.

The crystal structure of georgeericksenite has been solved by direct methods and refined to an R index of 3.5% using 2019 observed reflections measured with Mo$K\alpha$ X-radiation. There is one unique Cr site occupied by 0.84 Cr^{6+} + 0.16 S and tetrahedrally coordinated by four O atoms, one unique Mg site octahedrally coordinated by O atoms, three unique I sites octahedrally coordinated by O atoms and H_2O groups, three unique Na sites with octahedral, augmented octahedral and triangular dodecahedral coordinations, one unique Ca site with square antiprismatic coordination, and six unique (H_2O) groups. The cation polyhedra link by corner-, edge-, and face-sharing to form dense heteropolyhedral slabs parallel to (100); these slabs are linked by hydrogen bonding. The formula derived from the crystal-structure refinement is $Na_6CaMg(IO_3)_6[(Cr_{0.84}S_{0.16})O_4]_2(H_2O)_{12}$. Crystals of georgeericksenite are extremely unstable under the electron beam during electron microprobe analysis, and the analyzed amounts of all elements fluctuate strongly as a function of time and crystallographic orientation relative to the electron beam. However, extrapolation of the chemical composition to zero time yields values that are in reasonable accord with the chemical formula derived from crystal structure analysis.

INTRODUCTION

Georgeericksenite was first encountered as a potential new mineral species in 1984, when one of us (A.C.R.) was engaged in the acquisition of X-ray powder standards at the Pinch Mineralogical Museum, then situated in Rochester, New York. One particular specimen, labeled dietzeite from Oficina Chacabuco, Chile, had some bright lemon-yellow micronodules of crystals that gave an X-ray powder-diffraction pattern matching no data listed in the powder diffraction file for inorganic compounds, clearly indicating that the unknown could not be dietzeite. SEM energy-dispersion spectra contained major peaks for I, Ca, and Cr and minor peaks for Mg, Na, and S. The X-ray diffraction pattern and corresponding powder mount were set aside until the study was reopened in 1994. By this time, the mineral collections belonging to William W. Pinch had been purchased on behalf of the Canadian Museum of Nature and were located in Ottawa, Ontario, Canada. The specimen was retrieved and the ensuing mineralogical study was successful; the results are reported herein.

The new mineral is named for George E. Ericksen

0003–004X/98/0304–0390$05.00

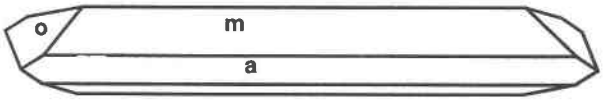

FIGURE 1. Idealized projection of a georgeericksenite crystal. $a = \{100\}, m = \{110\}, o = \{\bar{2}33\}$.

(1920–1996) of Reston, Virginia, who was a noted research economic geologist with the U.S. Geological Survey for fifty years. Among his many accomplishments, we wish to highlight his studies of the nitrate deposits of Chile that provided significant new information on the origin of saline accumulations in deserts. An outgrowth of this particular work led him to discover and help name six new minerals from Chile; fuenzalidaite, carlosruizite, and hectorfloresite are recently described I-bearing phases that bear his imprint. The mineral and mineral name have been approved by the Commission on New Minerals and Mineral Names (IMA). Holotype material, consisting of the specimen, polished thin section, and the crystal used for the structure determination are preserved in the Display Series of the National Mineral Collection of Canada at the Canadian Museum of Nature, Ottawa, Ontario, under catalog number CMNMI 82914.

DESCRIPTION

Occurrence and paragenesis

The locality label is Oficina Chacabuco, Chile. The coordinates of this locality are latitude 23°9′ S, longitude 69°37′ W. Nothing else about the pedigree of the specimen is known. It originally measured 5 × 4.5 × 3 cm and contains no more than 10 mg of georgeericksenite. The host rock is dirty light-gray-brown in color and is composed principally of halite, nitratine, and niter. Clasts of brown fine-grained plagioclase and black crystalline clinopyroxene are found embedded both in the matrix and in cavities. A second new mineral, an undefined hydrated Ca-K-Ti-iodate-chromate-chloride, occurs as small 0.1 mm sized fibrous tufts that protrude from small cavities and are also randomly scattered on the matrix. Individual crystals of this second phase are lemon yellow and acicular with a length-to-width ratio approaching 100:1. Further study of this phase is currently underway.

Georgeericksenite occurs as isolated or, in some cases, as groupings of bright lemon-yellow micronodules of crystals that are concentrated on the surface of one part of the mineral specimen. These micronodules average about 0.2 mm in size and each is composed of numerous individual crystals in random orientation. We can only speculate on the provenance, but it certainly seems to be the last mineral to form in this assemblage.

Mineral data

An idealized projection of a georgeericksenite crystal is shown in Figure 1; SEM photomicrograph of a part of an aggregate is given in Figure 2. The characteristics of the mineral are given in Table 1 and the fully indexed X-ray powder-diffraction pattern is given in Table 2.

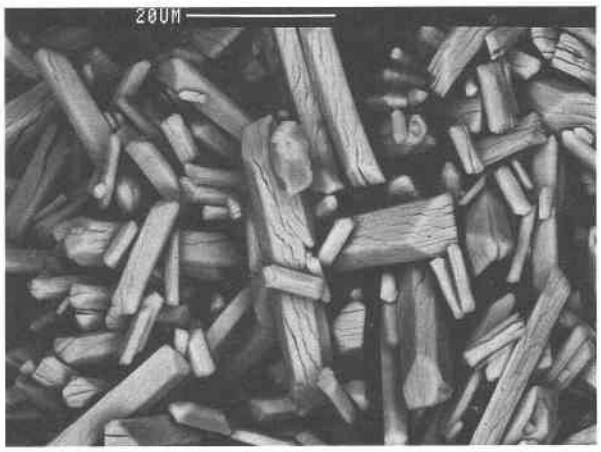

FIGURE 2. SEM photomicrograph of part of a georgeericksenite aggregate: scale bar = 20 μm, note the cracking of the crystals due to H_2O loss under the SEM vacuum.

A dearth of suitable crystals and the extreme solubility of the mineral combined to make the acquisition of complete optical properties virtually impossible. We could not mount or remove grains for spindle-stage work; all measurements are based on one grain. We could not measure 2 V for two reasons: (1) AB is the elongate axis (which unfortunately was not the orientation of the one grain suitable for measurement); (2) no extinction curves were usable as the crystal was attached to the side of a thin glass rod.

Electron microprobe examination

Two acicular crystals were attached to the surface of a plexiglas disk with epoxy. The disk was coated with carbon and carbon paint was then applied to the ends of the crystal. One crystal had the (100) surface uppermost; the other crystal had a growth face of the form {110} uppermost; we designate this as (110). Before analysis, the crystals were translucent. After analysis, the remnants were opaque and pitted and the crystal surface was stained brown (presumably by I_2).

The crystals were examined with a CAMECA SX-50 electron microprobe operating in wavelength-dispersive mode at 15 kV and various currents from 20 nA to 0.5 nA. The instrument has three spectrometers and the constituents were examined in the sequence (Na, Cr, I), then (Mg, S, Ca). For at least the first 200 s when the crystal was exposed to the electron beam, the counts per second on each element varied with time by up to an order of magnitude, indicating that the crystals are extremely unstable in the electron beam. In addition, the counts per second for each element at a given time are very dependent on the surface [(100) or (110)] analyzed. This behavior is summarized in Figure 3.

Over very short counting times (<10 s) at 15 kV and 5 nA, there is a drop in Na_2O and a gain in I_2O_5 relative to the ideal values. Other components approximate the ideal values, although a significant orientation effect ex-

TABLE 1. Descriptive characteristics of georgeericksenite

Physical properties	
Color	pale yellow (crystals) to bright lemon yellow (aggregates)
Streak	pale yellow
Luster	vitreous
Diaphaneity	transparent (crystals) to translucent (aggregates)
Fluorescence	none observed
Fracture	unknown
Hardness (Mohs)	3–4 (estimated)*
Density	3.035_{calc} g/cm³†
Tenacity	brittle
Cleavage	none observed
Solubility	extreme in cold H_2O
Morphology	
Habit	prismatic to acicular along [001] and somewhat flattened on {110}
General appearance	subhedral to euhedral
Forms	{100}, [110} major, and [$\bar{2}$33} minor
Crystal size	30 × 5 × 5 μm (average); up to 0.1 mm in longest dimension
Length-to-width ratio	6:1
Twinning	none observed megascopically nor during single-crystal study
Optical properties	
Indicatrix	biaxial positive
α	1.647(2)
β	1.674(2)
γ	1.704(2)
$2V_{calc}$	+88.4°
Orientation	$Z \approx c$
Pleochroism	slight; X = very pale yellow, Z = distinct yellow-green
Gladstone-Dale compatibility ($1 - K_p/K_c$)	0.021 (excellent)‡
Unit-cell data§	
Monoclinic, $C2/c$, $Na_6CaMg(IO_3)_6[(Cr_{0.84}S_{0.16})O_4]_2(H_2O)_{12}$	
a (Å)	23.645(2)
b (Å)	10.918(1)
c (Å)	15.768(1)
β (°)	114.42(6)
V (Å³)	3707.3(6)
Z	4
$a:b:c$	2.1657:1:1.4442

* Nodules are much softer than individual crystals.
† Derived from crystal-structure formula and unit-cell parameters.
‡ Crystal-structure formula and calculated density; k = 0.200 for MgO.
§ Derived from crystal-structure analysis.

ists for SO_3 and CaO, values for the (100) and (110) surfaces straddling the ideal values. With increasing exposure to the electron beam, Na_2O increases and all other oxides decrease, and this behavior is much more rapid on the (100) surface than on the (110) surface. After about 100 s, the oxide values show little further change on (100); the same occurs for the (110) surface after 200 s. The (100) surface seems to be more reactive to the electron beam than the (110) surface, but both surfaces seem to equilibrate with the beam and give comparatively similar oxide weight percent values after 200 s.

The variation in Na_2O as a function of time was further investigated at 15 kV and 1 nA. Counts were taken every 5 s without moving the beam and are shown in Figure 4. The lines fitted to the data points were extrapolated to zero time and the resulting values were converted to weight percent Na. For the (110) surface, the extrapolated value is 8 wt% Na, in close agreement with the ideal value of 8.15 wt% (in addition, there was a complementary rapid increase in counts for I in the first three counting periods). However, for the (100) surface, the extrapolated value of 1.6 wt% Na falls well below the ideal value of 8.15 wt%. Figure 3 indicates that the (100) surface responds more rapidly to the electron beam than the (110) surface. We conjecture that the (100) surface has lost Na during the first second or so in the beam and then continues to evolve as indicated in Figures 3 and 4.

Georgeericksenite is extremely unstable under the electron beam, even at low current and short counting times. The brown staining of the crystal is consistent with reaction with I_2 and the decrease in analyzed I_2O_5 with increasing time. Moreover, the analytical values at any given time are strongly dependent on the crystallographic orientation of the material analyzed. The overall quantitative behavior of georgeericksenite in the electron beam (as summarized in Figs. 3 and 4) is consistent with the chemical composition derived from crystal-structure refinement (ideally I_2O_5 59.13, CrO_3 9.92, SO_3 1.51, MgO 2.38, CaO 3.31, Na_2O 10.98, H_2O 12.77 wt%). However, it does not seem reasonable to use any compositions derived from electron-microprobe analysis considering the reactive nature of the crystals over even extremely short times.

TABLE 2. X-ray powder diffraction data for georgeericksenite

I_{obs}	d_{obs}	d_{calc}	I_{calc}	*hkl*	I_{obs}	d_{obs}	d_{calc}	I_{calc}	*hkl*
100	10.69	10.754	100	200	3	2.287	2.290	1	$\bar{6}26$
20	9.74	9.705	10	110	3	2.237	2.233	2	$\bar{2}44$
20	8.82	8.834	7	$\bar{1}11$	5	2.210	2.209	3	$\bar{4}44$*
		7.575	8	$\bar{2}02$	3	2.195	2.189	3	$\bar{6}43$
30	7.48								
		7.416	13	111			2.166	3	640
3	7.14	7.157	2	002			2.165	1	$\bar{10}23$
50	6.36	6.358	24	$\bar{3}11$			2.165	2	044
					20	2.159			
10	5.99	5.986	4	$\bar{3}10$			2.163	1	135
50	5.65	5.650	29	$\bar{3}12$			2.160	2	533
		5.377	5	400					
30	5.33						2.153	4	$\bar{10}22$
		5.307	9	112	5	2.128	2.129	2	$\bar{10}24$*
5	5.09	5.083	3	021	3	2.096	2.096	2	$\bar{3}51$
		4.948	1	311	10	2.078	2.083	3	$\bar{11}12$*
3	4.91								
		4.881	1	$\bar{2}21$	5	2.050	2.050	2	$\bar{6}27$
15	4.64	4.638	5	$\bar{1}13$*			2.024	6	$\bar{2}27$
					25	2.021			
40	4.36	4.355	19	221			2.023	3	$\bar{11}15$
25	3.909	3.915	16	$\bar{2}04$*			1.999	1	$\bar{8}42$
					10	1.996			
25	3.790	3.788	12	$\bar{4}04$*			1.995	1	930
		3.586	32	023			1.993	1	515
70	3.590								
		3.585	15	600	3	1.971	1.969	1	$\bar{3}35$
							1.968	1	$\bar{5}52$
30	3.524	3.533	12	$\bar{4}23$					
		3.518	12	511			1.958	3	$\bar{8}27$
30	3.453	3.450	13	421*	3	1.956			
							1.954	2	534
3	3.389	3.393	2	$\bar{5}14$	5	1.936	1.937	2	352*
		3.290	2	$\bar{1}32$	40	1.913	1.912	15	840*
10	3.296								
		3.290	3	$\bar{3}31$	40	1.887	1.886	12	$\bar{4}46$*
10	3.181	3.179	6	$\bar{3}32$*	30	1.848	1.845	7	$\bar{12}06$*
80	3.121	3.123	54	$\bar{2}23$*	20	1.819	1.822	3	$\bar{10}27$
80	3.051	3.054	58	$\bar{6}23$*			1.821	2	$\bar{1}18$
10	2.966	2.960	7	$\bar{1}33$*			1.818	2	$\bar{9}18$
		2.919	4	$\bar{5}15$			1.790	1	$\bar{11}35$
5	2.912				15	1.789			
		2.896	2	$\bar{1}15$			1.787	1	$\bar{3}55$
5	2.853	2.853	3	$\bar{5}32$*			1.767	1	$\bar{7}54$
					20	1.765			
5	2.765	2.761	3	332*			1.763	2	$\bar{2}62$
15	2.718	2.719	10	040*			1.762	2	$\bar{10}44$
10	2.685	2.688	8	800*	3	1.744	1.742	1	$\bar{10}41$
		2.636	5	240	5	1.721	1.723	2	$\bar{5}19$*
20	2.631								
		2.619	6	$\bar{4}06$			1.694	1	063
					15	1.691			
5	2.560	2.568	4	$\bar{8}23$			1.689	1	$\bar{4}63$
30	2.534	2.535	10	404*	10	1.650	1.650	3	$\bar{4}29$*
		2.469	2	$\bar{4}41$			1.637	5	263
10	2.465				30	1.635			
		2.462	1	$\bar{9}14$			1.634	6	1023
5	2.419	2.415	1	712*	5	1.626	1.627	4	$\bar{6}63$*
15	2.375	2.380	4	$\bar{5}32$*			1.602	4	$\bar{2}29$
					35	1.602			
30	2.322	2.327	6	$\bar{9}15$*			1.598	6	$\bar{14}25$

Note: 114.6 mm Debye-Scherrer camera, Cu$K\alpha$ (Ni-filtered) radiation, observed intensities visually estimated, calculated intensities obtained from structure data; not corrected for shrinkage and no internal standard. Indices marked with an asterisk were not used for unit-cell refinement. Unit-cell parameters refined from powder data are: a = 23.62(2), b = 10.875(5), c = 15.72(1) Å, β = 114.42(6)°.

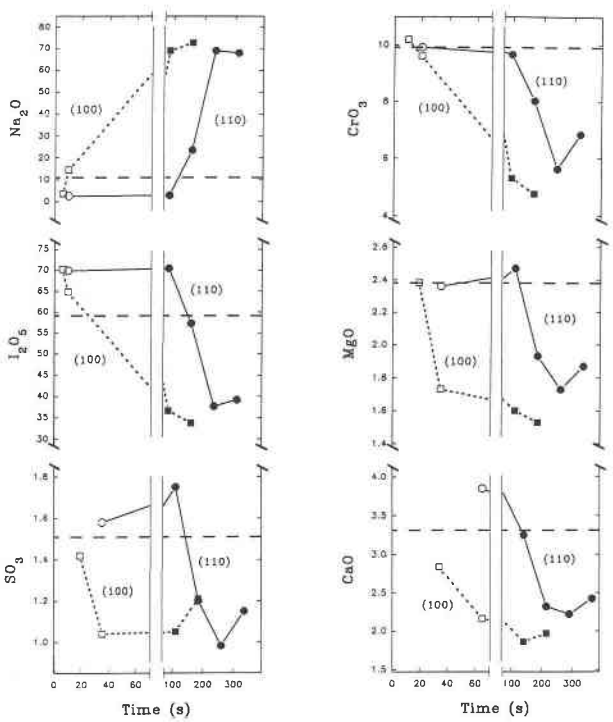

FIGURE 3. Variation in constituents in weight percent as a function of time (increasing exposure of the crystal to the electron beam); note that the data points do not necessarily correspond to the same times as not all elements were acquired simultaneously. The dashed horizontal lines correspond to the weight percent values indicated by the chemical composition derived from crystal-structure analysis.

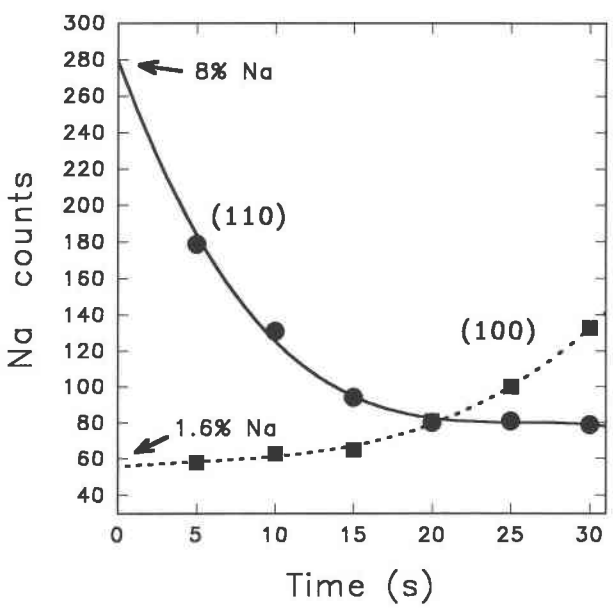

FIGURE 4. Variation in counts for Na in georgeericksenite as a function of time for the (100) and (110) surfaces; the number of counts corresponding to 8 wt% Na is indicated.

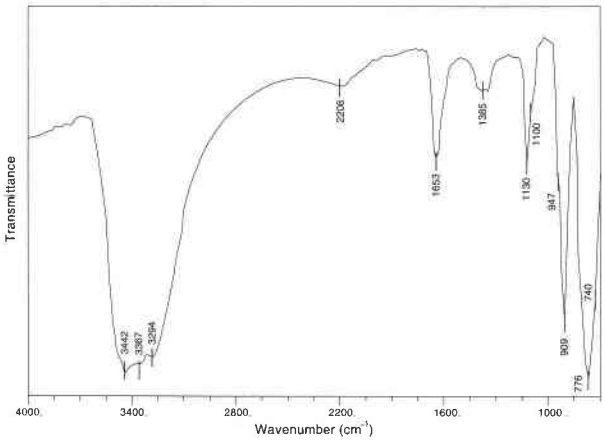

FIGURE 5. Infrared-transmission spectrum for georgeericksenite.

Infrared study

The equipment and procedures for acquiring the infrared spectrum for powdered georgeericksenite dispersed in KBr are identical to those used to obtain the spectrum for mcalpineite (Roberts et al. 1994). A very strong absorption band (Fig. 5), which stretches from 3442 to 3294 cm^{-1} and is centered at 3367 cm^{-1}, is due to O-H stretching, and a medium band, centered at 1653 cm^{-1}, is due to H-O-H bending in the H_2O groups. The iodate groups are characterized by strong bands at 740 (v_1) and 776 (v_3) cm^{-1} which are stretching vibrations. The chromate groups are characterized by two bands at 909 (strong) and 947 (medium) cm^{-1}, which are both stretching vibrations (Nakamoto 1978).

Crystal structure

Data collection

A 0.046 × 0.059 × 0.060 mm^3 crystal was mounted on a Siemens *P*4 automated four-circle diffractometer and aligned using 42 reflections automatically centered following measurement from a rotation photograph. Mo*K*α radiation was used. The orientation matrix and unit-cell dimensions (Table 1) were determined from the setting angles by least-squares refinement. A total of 3872 unique reflections was collected out to 60° 2θ with a fixed scan speed of 1.33° 2θ/min. We corrected for absorption by Gaussian quadrature integration; corrected for Lorentz, polarization, and background effects; and reduced the intensities to structure factors. Of the 3872 unique reflections, 2019 were classed as observed ($|F_o|>5\sigma|F_o|$).

Structure solution and refinement

All calculations were done with the SHELXTL PC Plus system of programs; *R* and *Rw* indices are of the conventional form: $R = \Sigma(|F_o|-|F_c|)/\Sigma|F_o|$ and $Rw = [\Sigma w(|F_o|-|F_c|)^2/\Sigma F_o^2]^{1/2}$. The value for the absorption coefficient $\mu(mm^{-1})$ is 5.86; min. transmission is 0.734; and max. transmission is 0.827. The structure was solved by direct methods. The *E* statistics indicate that the structure is probably centrosymmetric, and systematic absences in-

TABLE 3. Final atomic parameters for georgeericksenite

Site	*x*	*y*	*z*	U_{eq}	U_{11}	U_{22}	U_{33}	U_{23}	U_{13}	U_{12}
Ca	0	0.1223(3)	¼	16(1)	16(2)	14(2)	14(2)	0	2(1)	0
Mg	½	0.1056(5)	¼	15(2)	23(3)	12(3)	13(3)	0	11(2)	0
Na1	0.1379(2)	0.1783(5)	0.1780(3)	27(2)	29(3)	28(3)	25(3)	−1(2)	13(2)	3(3)
Na2	0.1228(2)	0.3922(5)	0.3304(3)	25(2)	26(3)	22(3)	22(2)	−3(2)	5(2)	1(2)
Na3	0.3777(2)	0.1291(5)	0.0189(4)	34(2)	30(3)	33(3)	37(3)	0(3)	12(2)	−4(3)
I1	0.12628(3)	0.11870(7)	0.49298(5)	162(3)	164(4)	153(4)	143(4)	18(4)	38(3)	7(3)
I2	0.00440(3)	0.37451(7)	0.08827(5)	133(3)	149(4)	137(4)	111(3)	−9(3)	53(3)	−8(3)
I3	0.36796(3)	0.15586(7)	0.29555(5)	179(3)	177(4)	181(4)	175(4)	−3(4)	69(3)	41(4)
Cr	0.4843(1)	0.3465(2)	0.0852(1)	14(1)	16(1)	12(1)	13(1)	−1(1)	4(1)	1(1)
O1	0.3272(4)	0.2589(7)	0.4317(5)	23(3)	22(5)	24(5)	18(4)	−3(4)	4(4)	−5(4)
O2	0.1789(4)	0.0616(8)	0.4456(6)	30(4)	27(5)	35(5)	31(5)	−1(4)	14(4)	11(5)
O3	0.0786(4)	0.2143(7)	0.3950(5)	19(3)	19(5)	16(4)	15(4)	5(4)	0(4)	3(4)
O4	0.0511(3)	0.2896(8)	0.1928(5)	18(3)	14(4)	27(5)	11(4)	4(4)	2(3)	4(4)
O5	0.0336(3)	0.4799(7)	0.3624(5)	20(3)	15(4)	27(5)	15(4)	6(4)	4(4)	−4(4)
O6	0.0630(4)	0.4704(7)	0.0767(5)	22(3)	13(4)	24(5)	26(5)	−1(4)	5(4)	−7(4)
O7	0.3272(4)	0.2846(8)	0.2247(6)	32(4)	43(6)	22(5)	24(5)	3(4)	7(4)	23(4)
O8	0.3081(4)	0.0427(9)	0.2601(7)	49(5)	23(5)	53(7)	55(7)	26(6)	1(5)	−9(5)
O9	0.4075(4)	0.0991(8)	0.2278(5)	28(3)	32(5)	41(6)	17(4)	3(4)	16(4)	18(4)
O10	0.0614(4)	0.1818(9)	0.0206(6)	40(4)	40(6)	49(7)	20(4)	−11(5)	1(4)	9(5)
O11	0.4772(6)	0.2344(9)	0.1450(7)	56(6)	90(9)	32(6)	52(7)	15(5)	36(7)	−4(6)
O12	0.4668(4)	0.4759(8)	0.1204(6)	30(4)	30(5)	25(5)	26(5)	−8(4)	3(4)	−1(4)
O13	0.4446(4)	0.3503(9)	0.4038(7)	49(5)	25(5)	56(7)	69(7)	14(6)	21(5)	−1(5)
OW1	0.0975(4)	0.0281(8)	0.2522(6)	32(4)	38(6)	21(5)	38(5)	−4(4)	18(5)	5(4)
OW2	0.1947(4)	0.3370(9)	0.1437(5)	32(4)	44(6)	28(5)	24(5)	7(4)	14(4)	−2(5)
OW3	0.1982(4)	0.2442(8)	0.3359(6)	27(4)	20(5)	31(6)	33(5)	−7(4)	13(4)	4(4)
OW4A	0.1895(7)	−0.003(1)	0.167(1)	27(3)†	—	—	—	—	—	—
OW4B	0.1979(6)	0.063(2)	0.118(1)	27(3)†	—	—	—	—	—	—
OW5	0.1865(4)	0.4556(8)	0.4851(6)	27(4)	32(5)	26(5)	24(5)	−7(4)	12(4)	−1(4)
OW6	0.3130(5)	0.2809(9)	0.0420(7)	42(4)	50(7)	43(6)	41(6)	11(5)	27(5)	4(6)

Note: *U* values are ×10^3 except for Iodine, which are 10^4.
† Isotropic and constrained to be equal.

TABLE 5. Selected interatomic distances (Å) and angles (°) in georgeericksenite

Ca polyhedron		**Mg octahedron**	
Ca-O3,b	2.485(7) ×2	Mg-O5c,d	2.119(8) ×2
Ca-O4,b	2.552(9) ×2	Mg-O9,h	2.068(9) ×2
Ca-O12d,i	2.454(9) ×2	Mg-O11,h	2.07(1) ×2
Ca-OW1,b	2.51(1) ×2	⟨Mg-O⟩	2.09
⟨Ca-O⟩	2.50		
Na1 polyhedron		**Cr tetrahedron**	
Na1-O4	2.48(1)	Cr-O10f	1.597(8)
Na1-O10	2.393(8)	Cr-O11	1.60(1)
Na1-OW1	2.43(1)	Cr-O12	1.633(9)
Na1-OW2	2.39(1)	Cr-O13h	1.62(1)
Na1-OW3	2.411(9)	⟨Cr-O⟩	1.61
Na1-OW4A	2.37(2)		
Na1-OW4B	2.37(2)	**I1 pyramid**	
⟨Na1-O⟩	2.41	I1-O1a	1.824(7)
Na2 polyhedron		I1-O2	1.81(1)
Na2-O3	2.60(1)	I1-O3	1.819(7)
Na2-O4	2.407(8)	⟨I1-O⟩	1.82
Na2-O5	2.55(1)	**I2 pyramid**	
Na2-O8g	3.06(1)	I2-O4	1.814(7)
Na2-O9g	2.43(1)	I2-O5b	1.820(9)
Na2-OW3	2.38(1)	I2-O6	1.806(9)
Na2-OW5	2.378(8)	⟨I2-O⟩	1.81
⟨Na2-O⟩	2.54		
Na3 polyhedron		**I3 pyramid**	
Na3-O5d	2.704(8)	I3-O7	1.806(8)
Na3-O6f	2.68(1)	I3-O8	1.786(9)
Na3-O9	3.09(1)	I3-O9	1.80(1)
Na3-O10f	2.73(1)	⟨I3-O⟩	1.80
Na3-O11	2.64(1)		
Na3-OW2f	2.453(8)		
Na3-OW5d	2.41(1)		
Na3-OW6	2.38(1)		
⟨Na3-O⟩	2.64		

Long Iodine Bonds

I1-O12d	2.686(8)	I2-O3b	2.722(9)	I3-O1	2.92(1)
I1-O13a	2.80(1)	I2-O6e	2.957(7)	I3-O6d	2.846(7)
I1-OW4Aj	2.82(2)	I2-O10	2.93(1)	I3-O13	2.854(9)
I1-OW4Bj	2.81(2)	⟨I2-O⟩	2.87	⟨I3-O⟩	2.87
⟨I1-O⟩	2.77				
OW4A-OW4B	1.13(3)				

Note: Symmetry operators: a = $\bar{x}$ + ½, $\bar{y}$ + ½, $\bar{z}$ + 1; b = $\bar{x}$, *y*, $\bar{z}$ + ½; c = *x* + ½, *y* − ½, *z*; d = $\bar{x}$ + ½, *y* − ½, $\bar{z}$ + ½; e = $\bar{x}$, $\bar{y}$ + 1, $\bar{z}$; f = $\bar{x}$ + ½, $\bar{y}$ + ½, $\bar{z}$; g = $\bar{x}$ + ½, *y* + ½, $\bar{z}$ + ½; h = $\bar{x}$ + 1, *y*, $\bar{z}$ + ½; i = *x* − ½, *y* − ½, *z*; j = *x*, $\bar{y}$, *z* + ½.

dicate the presence of a *c* glide for the *C*-centered cell. The solution with the highest combined figure-of-merit in the space group *C*2/*c* proved to be correct, and the structure was refined by a combination of least-squares refinement and difference-Fourier synthesis to an *R* index of 3.5% and *Rw* = 3.5%. Site occupancies were assigned on the basis of site-scattering refinement and crystal-chemical criteria. Final atomic parameters are listed in Table 3, observed and calculated structure-factors are listed in Table 4[1] and selected interatomic distances and angles are given in Table 5. A bond-valence analysis is shown in Table 6.

[1] For a copy of Table 4, Document AM-98-006, contact the Business Office of the Mineralogical Society of America (see inside front cover of recent issue) for price information. Deposit items may also be available on the American Mineralogist web site (see inside back cover of a current for web address).

DESCRIPTION OF THE STRUCTURE

Cation coordination

The one symmetrically distinct Cr site is tetrahedrally coordinated by four O atoms at a mean distance of 1.61 Å, indicating that the Cr cation is hexavalent. The observed site-scattering and the mean bond-length at the Cr site are less than that expected for complete occupancy by Cr^{6+}. This can be accounted for by some substitution of S. Hence the occupancy of the Cr site was considered variable (Cr, S) and site-scattering refinement converged to an occupancy of 0.84(2) Cr + 0.16(2) S. This value is in accord with the observed ⟨Cr-O⟩ distance and detection of S with an electron microprobe.

Each of the three I sites is coordinated by three O atoms arranged in a triangle to one side of the cation and at distances of ~1.81 Å, such that the resulting IO_3 group constitutes a triangular pyramid with the I site at the apex of the pyramid (Fig. 6). For each site, there are three additional ligands (Table 5, Fig. 6) such that the I atoms have very distorted octahedral coordination and occupy off-centered positions within each octahedron. The I1 site is coordinated by one H_2O group, OW4, that shows positional disorder (Fig. 6) but the coordination is similar to that of the other I polyhedra. This type of eccentric coordination is typical for I^{5+} with a stereoactive lone-pair of electrons. Note that the long bonds still contribute significant bond-valence (~0.20 v.u. per bond) to the bonded anions.

There are three unique Na sites (Fig. 6, Table 5), each with a different type of coordination. Na1 is surrounded by two O atoms and four H_2O groups in a distorted octahedral arrangement with a ⟨Na1-ϕ⟩ distance (ϕ = unspecified ligand) of 2.41 Å. Na2 is surrounded by five O atoms and two H_2O groups in an augmented octahedral arrangement with a ⟨Na2-ϕ⟩ distance of 2.54 Å. Na3 is surrounded by five O atoms and three H_2O groups in a triangular dodecahedral arrangement with a ⟨Na3-ϕ⟩ distance of 2.64 Å. The variation in ⟨Na-ϕ⟩ distance as a function of coordination number is in accord with the radii of Na given by Shannon (1976).

There is one Mg site coordinated by six O atoms in an octahedral arrangement with a ⟨Mg-O⟩ distance of 2.09 Å; the site-scattering and observed mean bond-length are in accord with this site being occupied by Mg. There is one Ca site coordinated by six O atoms and two H_2O groups in a square-antiprismatic arrangement (Fig. 7) with a ⟨Ca-ϕ⟩ distance of 2.50 Å. The observed site-scattering and mean bond-length indicate that this site is completely occupied by Ca.

Structure topology

The structural arrangement in georgeericksenite consists of thick slabs of polyhedra orthogonal to [100] (Fig. 8). These slabs have the composition of the mineral and are one-half a unit cell thick in the [100] direction; linkage with adjacent slabs is solely by hydrogen bonding. Although the slab appears complicated when viewed

TABLE 6. Bond-valence* table for georgeericksenite, omitting the H atoms bonded to O4A and O4B

	Ca	Mg	Cr	Na1	Na2	Na3	I1	I2	I3	H3	H4	H5	H6	H9	H10	H11	H12	Σ
O1							1.40		0.17			0.20		0.20				1.97
O2							1.45						0.20		0.15			
O3	0.25 ×2↓				0.12		1.42	0.23										2.02
O4	0.21 ×2↓			0.16	0.18			1.44										1.99
O5		0.32 ×2↓			0.13	0.09		1.42										1.96
O6						0.10		1.47	0.19									1.92
O7									1.47	0.15						0.20		
O8					0.04				1.54		0.20							
O9		0.36 ×2↓			0.17	0.04			1.49									2.06
O10			1.60	0.19		0.09		0.17										2.05
O11		0.36 ×2↓	1.59			0.11												2.06
O12	0.27 ×2↓		1.45				0.25											1.97
O13			1.51				0.20		0.19									1.90
OW1	0.23 ×2↓			0.17														
OW2				0.19		0.17				0.85	0.80							2.01
OW3				0.18	0.20							0.80	0.80					1.98
OW4A				0.10			0.10											
OW4B				0.10			0.10											
OW5					0.20	0.18								0.80	0.85			2.03
OW6						0.20										0.80	0.80	2.00
Σ	1.92	2.08	6.15	1.09	1.04	0.98	4.92	4.89	5.05	1.00	1.00	1.00	1.00	1.00	1.00	1.00	1.00	

* Bond-valence curves from Brown and Altermatt (1985) for Ca, Cr, S, and from Brown (1981) for Mg, Na, and I.

down the *c* axis (Fig. 8), one sees that the edges of the slab are bounded by near-planar layers of anions. Further inspection shows that there are three planar layers of cations within the slab and parallel to its edges, indicating that the slab consists of three layers of polyhedra. The top and bottom of the slab are related by *c*-glide symmetry, and hence the slab may be factored into two distinct sheets of polyhedra, illustrated in Figure 9.

The outer layer of the slab (Fig. 9a) contains prominent zigzag chains of Na polyhedra extending along the *c* direction. The Na1 octahedron shares an edge with the Na2 augmented octahedron, which shares a face with the Na3 triangular dodecahedron to form a linear trimer that extends approximately in the [011] direction. This trimer links by edge-sharing between the Na3 and Na1 polyhedra to another trimer extending in the [0$\bar{1}$1] direction. This motif continues to form an $[Na_3\phi_{14}]$ zigzag chain

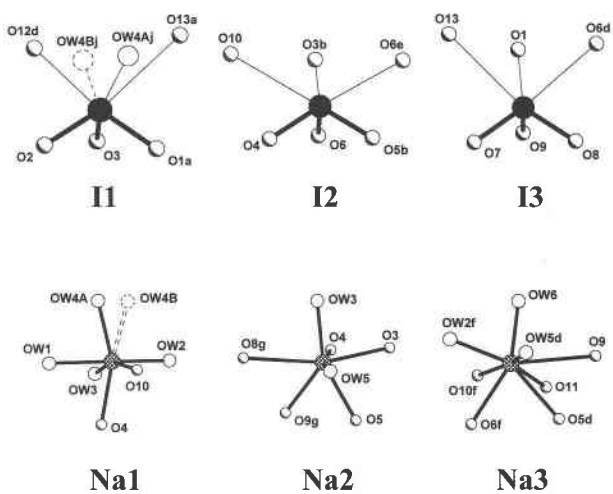

FIGURE 6. The coordination environments of the I and Na sites in georgeericksenite; I = large black circles; Na = cross-hatched circles; O = highlighted circles; H_2O = unshaded circles. One of the bonds to the disordered OW4 H_2O group is shown as a broken line.

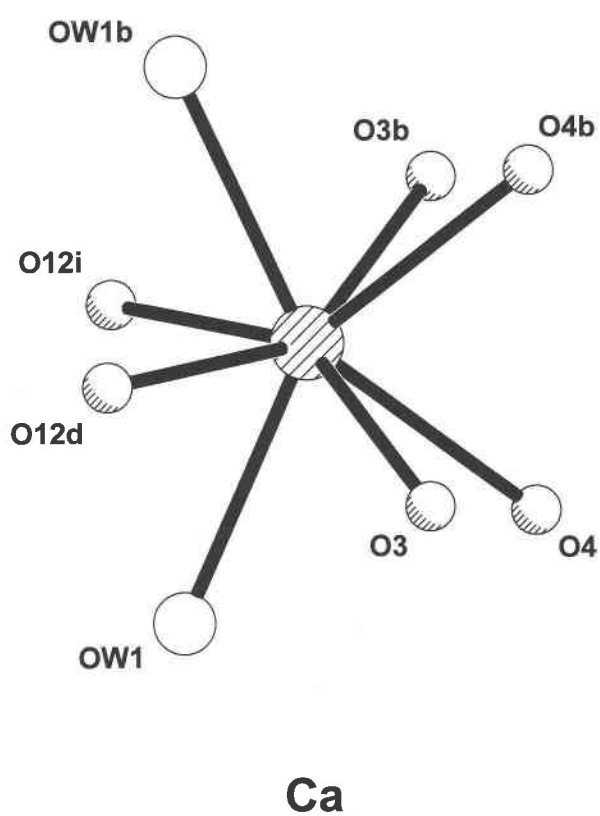

FIGURE 7. The coordination environment of the Ca site in georgeericksenite; Ca = diagonal-lined circle; legend as in Figure 6.

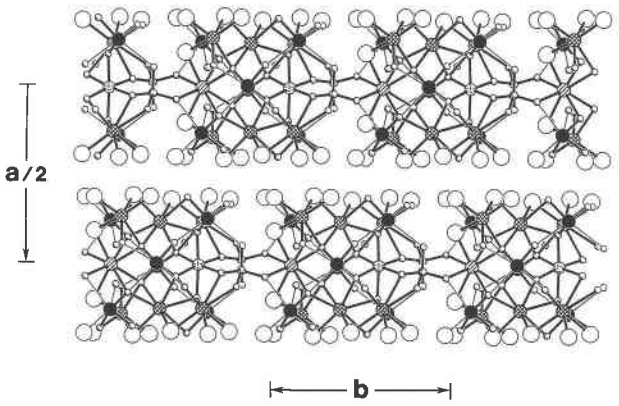

FIGURE 8. The crystal structure of georgeericksenite projected along [001]; legend as in Figures 6 and 7.

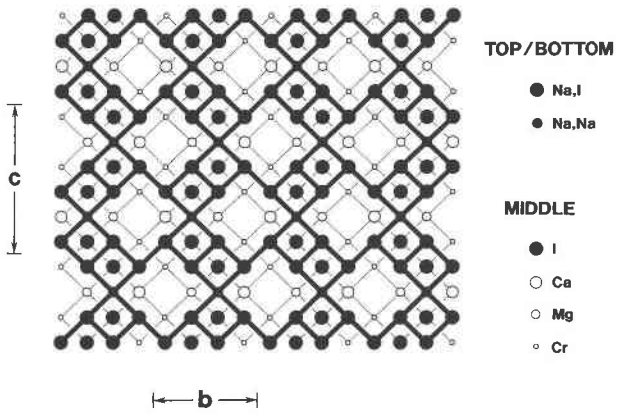

FIGURE 10. The cation array of the slab in georgeericksenite projected down [100]. The cations occupy the vertices of 4^4 plane nets, and the occupied vertices are joined by edges of the nets. The top and bottom nets superimpose (the heavy black lines) and the middle net (the dotted lines) is out of registry with the top and bottom nets.

extending in the c direction (Fig. 9a). In each embayment of this chain, the polyhedra are decorated by two (IO_{3+3}) groups. This outer layer of the slab consists of translationally equivalent decorated chains parallel to c that link only through one (unique) weak I-O bond. (Fig. 9a). The inner layer of the slab (Fig. 9b) consists of one unique Mg octahedron that shares corners with two Cr tetrahedra to form an [$MT_2\phi_{12}$] cluster (Hawthorne 1985). The other two meridional anions of the Mg octahedron link by corner-sharing to two (IO_{3+3}) groups (both involving the I2 site). These [$Mg(CrO_4)_2(IO_{3+3})_2O_2$] clusters link together two ($Ca\phi_8$) polyhedra to form chains parallel to the b axis (Fig. 9b). These chains link by weak I-O bonds to form the central layer of the slab.

The relations between the outer layers (Fig. 9a) and inner layer (Fig. 9b) of the slab is illustrated in Figure 10, which shows only the cation positions in each layer for clarity. All cations occupy the vertices of a 4^4 net, and occupied vertices are joined by the edges of each net in Figure 10. In the middle layer, all vertices are occupied by cations (I, Ca, Mg, and Cr), and the edges joining the occupied vertices are shown as dotted lines. In the top and bottom layers, only some of the vertices are occupied by cations, and the edges joining the occupied vertices are shown as heavy full lines. The top and bottom patterns of occupied vertices are almost exactly in registry but the chemical identities of occupied vertices that overlap (in projection) are different: vertices that contain Na

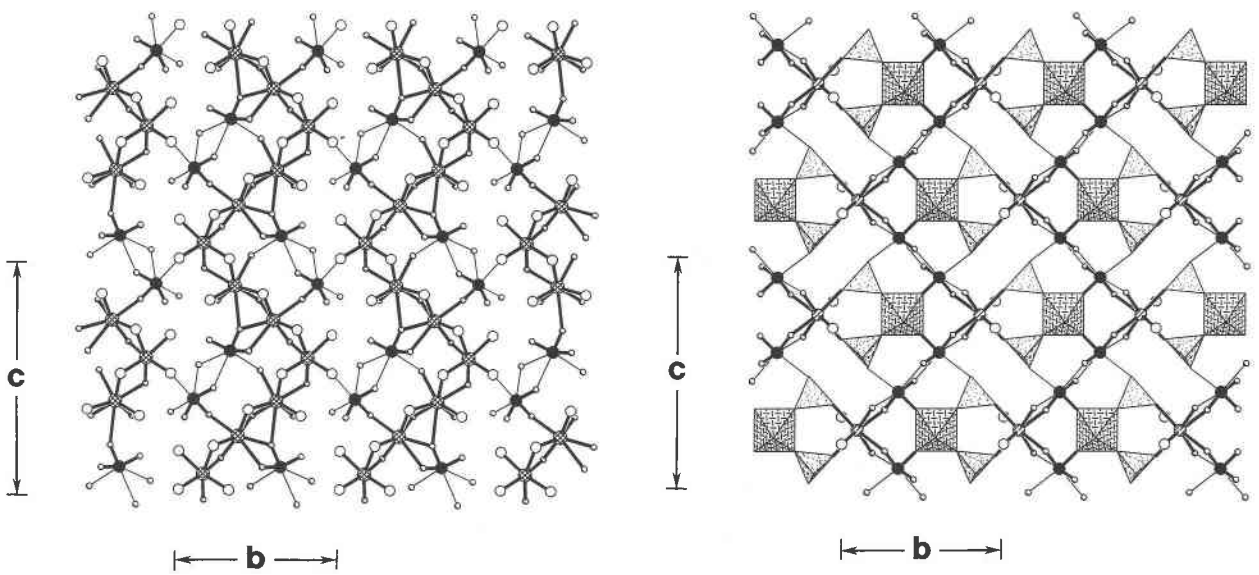

FIGURE 9. The crystal structure of georgeericksenite projected down [100]; legend as in Figures 6 and 7, plus Mg octahedron dash-shaded and Cr tetrahedron random-dot-shaded; (**left**) the outer layer(s) of the slab shown in Figure 8; (**right**) the inner layer of the slab shown in Figure 8.

TABLE 7. Bond-valence table for georgeericksenite: the disordered H_2O groups

		OW4A					OW4B				
	Σ	H1	H2	H7	H8	Σ	H1	H2	H7	H8	Σ
O1	1.97										
O2		0.20				2.00	0.20			0.05	2.05
O3	2.02										
O4	1.99										
O5	1.96										
O6	1.92										
O7					0.15	1.97		0.10			1.92
O8				0.20		1.98			0.20		1.98
O9	2.06										
O10	2.05										
O11	2.06										
O12	1.97										
O13	1.90										
OW1		0.80	0.85			2.05	0.80	0.90			2.10
OW2	2.01									0.05	2.06
OW3	1.98										
OW4A			0.15	0.80	0.85	2.00					
OW4B									0.80	0.90	1.90
OW5	2.03										
OW6	2.00										
Σ		1.00	1.00	1.00	1.00		1.00	1.00	1.00	1.00	

Note: Bond-valence curves from Brown and Altermatt (1985) for Ca, Cr, S, and from Brown (1981) for Mg, Na, and I.

in one layer and I in the other layer are shown as large black circles, and vertices that contain Na in both top and bottom layers are shown as small black circles. Note that the middle net is out of registry with the top and bottom nets by one half of the diagonal of the unit cell of the net. Thus, despite the complexity of each of the layers (Figs. 9a and 9b) of the slab, the layers mesh in an orderly geometric manner.

H_2O groups

The H atoms were not located in the final stages of the refinement. However, H_2O groups were identified by the bond-valence distributions in the structure (Table 6), and a reasonable hydrogen-bonding scheme was derived from bond valence and stereochemical criteria (Tables 7 and 8). There are six unique H_2O groups, labeled OW; during the final stages of refinement, the displacement parameters of the OW4 group were very anisotropic, and it was modeled as a positionally disordered (split) site, labeled OW4A and OW4B. These split positions refined to a separation of 1.13 Å. The reason for this disorder is not clear, although the two sites do show a different hydrogen-bonding arrangement (Table 8).

TABLE 8. Proposed hydrogen-bonding for georgeericksenite

ϕ-ϕ	(Å)	H-atom	ϕ-ϕ-ϕ	(°)
OW1 . . . O2	2.88(1)	H1	O2-OW1-OW4A	101.3(4)
OW1 . . . OW4A	3.01(2)	H2	O2-OW1-O7d	83.4(3)
OW1 . . . O7d	3.14(1)	H2′	OW4A-OW1-O7d	58.4(4)
*OW2 . . . O7	2.91(1)	H3	O7-OW2-O8g	100.8(3)
OW2 . . . O8g	2.73(1)	H4		
*OW3 . . . O1	2.79(1)	H5	O1-OW3-O2	97.4(3)
OW3 . . . O2	2.80(1)	H6		
*OW4A . . . O8	2.62(2)	H7	O8-OW4A-O7d	101.0(5)
OW4A . . . O7d	3.00(2)	H8		
*OW4B . . . O8	2.65(2)	H7′	O8-OW4B-O2	118.2(8)
OW4B . . . O2	2.90(2)	H8′	O8-OW4B-OW2	92.1(6)
OW4B . . . OW2	3.03(2)	H8″	O2-OW4B-OW2	125.9(7)
OW5 . . . O1a	2.77(1)	H9	O1a-OW5-O2a	95.2(3)
*OW5 . . . O2a	2.91(1)	H10		
OW6 . . . O7	2.76(1)	H11	O7-OW6-OW6f	98.3(6)
*OW6 . . . OW6f	2.80(2)	H12		

* Hydrogen bonding across structural units; symmetry operators as in Table 5.

Chemical composition

The observed site-scattering and local stereochemistry at each site in georgeericksenite enable us to write an accurate chemical formula for this mineral: $Na_6CaMg(IO_3)_6[(Cr_{0.84}S_{0.16})O_4]_2(H_2O)_{12}$. This is particularly important for georgeericksenite as the crystals are extremely unstable under an electron beam. However, projecting the evolution of analyzed component as a function of time back to zero time for each element detected by electron microprobe analysis (Figs. 3 and 4) does show reasonable agreement with the chemical formula derived by crystal-structure analysis.

Relation to other minerals

Dietzeite, $Ca(IO_3)_2(CrO_4)(H_2O)$, (Burns and Hawthorne 1993) is the only other chromate-iodate mineral. However, dietzeite has a heteropolyhedral framework structure of very different connectivity and shows no structural relation to georgeericksenite. Fuenzalidaite and carlosruizite (Konnert et al. 1994) are sulphate-iodates from Oficina Santa Luisa in the Chilean nitrate fields, and contain small amounts of Cr (~1 wt% CrO_3) substituting for S. They are also sheet structures, but the sheets are significantly different in connectivity from georgeericksenite.

ACKNOWLEDGMENTS

We thank William M. Pinch and George Robinson for their cooperation in supplying material for this work, Ron Chapman for his assistance with

the electron microprobe work, and Peter C. Burns and an anonymous reviewer for their comments on the manuscript. F.C.H. was supported by Natural Sciences and Engineering Research Council of Canada Operating and Major Equipment Grants.

References cited

Brown, I.D. (1981) The bond-valence method: an empirical approach to chemical structure and bonding. In M. O'Keeffe and A. Navrotsky, Eds., Structure and Bonding in Crystals: II. Academic Press, New York, 1–30.

Brown, I.D. and Altermatt, D. (1985) Bond-valence parameters obtained from a systematic analysis of the inorganic crystal structure database. Acta Crystallographica, B41, 244–247.

Burns, P.C. and Hawthorne, F.C. (1993) The crystal structure of dietzeite, $Ca_2H_2O(IO_3)_2(CrO_4)$, a heteropolyhedral framework mineral. Canadian Mineralogist, 31, 313–319.

Hawthorne, F.C. (1985) Towards a structural classification of minerals: The $^{VI}M^{IV}T_2\Phi_n$ minerals. American Mineralogist, 70, 455–473.

Konnert, J.A., Evans, H.T., Jr., McGee, J.J., and Ericksen, G.E. (1994) Mineralogical studies of the nitrate deposits of Chile: VII. Two new saline minerals with the composition $K_6(Na,K)_4Na_6Mg_{10}(XO_4)_{12}(IO_3)_{12}\cdot 12H_2O$: Fuenzalidaite (X = S) and carlosruizite (X = Se). American Mineralogist, 79, 1003–1008.

Nakamoto, K. (1978) Infrared and Raman spectra of inorganic and coordination compounds. Wiley, New York.

Roberts, A.C., Ercit, T.S., Criddle, A.J., Jones, G.C., Williams, R.S., Cureton, F.F., and Jensen, M.C. (1994) Mcalpineite, $Cu_3TeO_6\cdot H_2O$, a new mineral from the McAlpine mine, Tuolumne County, California, and from the Centennial Eureka mine, Juab County, Utah. Mineralogical Magazine, 58, 417–424.

Manuscript received May 27, 1997
Manuscript accepted November 6, 1997